AGU PUBLICATIONS

Geophysical Research Letters

RESEARCH LETTER
10.1002/2017GL074087

Key Points:
- Variability of open-ocean deep convection varies widely among climate models with implications reaching beyond the Southern Ocean
- Stratification influences the timescale of deep-convection variability in these models
- Sea ice volume affects the models' predominant regime: convective or nonconvective

Supporting Information:
- Supporting Information S1

Correspondence to:
A. Reintges,
areintges@geomar.de

Citation:
Reintges, A., T. Martin, M. Latif, and W. Park (2017), Physical controls of Southern Ocean deep-convection variability in CMIP5 models and the Kiel Climate Model, *Geophys. Res. Lett.*, *44*, 6951–6958, doi:10.1002/2017GL074087.

Received 11 OCT 2016
Accepted 8 JUN 2017
Accepted article online 16 JUN 2017
Published online 3 JUL 2017

Physical controls of Southern Ocean deep-convection variability in CMIP5 models and the Kiel Climate Model

A. Reintges[1], T. Martin[1], M. Latif[1,2], and W. Park[1]

[1]GEOMAR Helmholtz Centre for Ocean Research Kiel, Kiel, Germany, [2]University of Kiel, Kiel, Germany

Abstract Global climate models exhibit large biases in the Southern Ocean. For example, in models Antarctic bottom water is formed mostly through open-ocean deep convection rather than through shelf convection. Still, the timescale, region, and intensity of deep-convection variability vary widely among models. We investigate the physical controls of this variability in the Atlantic sector of the Southern Ocean, where most of the models simulate recurring deep-convection events. We analyzed output from 11 exemplary CMIP5 models and four versions of the Kiel Climate Model. Of the several potential physical control parameters that we tested, the ones shared by all these models are as follows: Stratification in the convection region influences the timescale of the deep-convection variability; i.e., models with a strong (weak) stratification vary on long (short) timescales. Also, sea ice volume affects the modeled mean state in the Southern Ocean: Large (small) sea ice volume is associated with a nonconvective (convective) predominant regime.

1. Introduction

Variability in the Southern Ocean on multidecadal and longer timescales is hardly detectable in observations owing to a too short instrumental record. Hints for the existence of long-term internal Southern Ocean variability on multidecadal and longer timescales are indicated by reconstructions based on, for instance, tree ring records [*Lara and Villalba*, 1993; *Cook et al.*, 2000; *Villalba et al.*, 2012] and Antarctic ice core and sediment records [e.g., *Jones et al.*, 2016]. Climate models provide an opportunity to learn more about long-term variability in the Southern Ocean. Control simulations that cover hundreds or thousands of years reveal variability modes in the Southern Ocean: In the Kiel Climate Model (KCM), a global ocean-atmosphere-sea ice model, it is shown that the Atlantic Meridional Overturning Circulation exhibits a quasiperiodic multicentennial variability that is driven by Southern Ocean processes [*Park and Latif*, 2008]. In further studies based on the KCM, the multicentennial variability mode is reported also for the Southern Ocean sea surface temperature (SST) and is related to the onset and shutdown of Southern Ocean deep convection [*Martin et al.*, 2013; *Latif et al.*, 2013].

Open-ocean deep-convection events are rarely observed in the Southern Ocean. Satellite-based ice observations were launched in 1972, and since then, only one major event occurred: During the three consecutive winters of 1974 to 1976, an open-ocean polynya—an ice-free area surrounded by sea ice—of roughly 250,000 km^2 appeared [*Carsey*, 1980; *Gordon*, 2014]. Observations suggest that Antarctic bottom water is mainly formed at the Antarctic continental margins [*Orsi et al.*, 1999]. However, ocean and climate models have difficulties to simulate the processes at the Antarctic shelf due to their small spatial scales [*Heywood et al.*, 2014]. In models, Antarctic bottom water is typically formed by open-ocean deep convection which may cause biases in Southern Ocean [*Heuzé et al.*, 2013]. The ability of the models participating in the Coupled Model Intercomparison Project phase five (CMIP5) to capture the observed bottom water properties and the recent trend in sea ice is limited [*Heuzé et al.*, 2013; *Zunz et al.*, 2013], and different strengths of deep convection are simulated [*de Lavergne et al.*, 2014] with consequences for the ventilated water volume [*Behrens et al.*, 2016]. In many models, the simulated mixed layer is too warm, too light, and too shallow which leads to an increased stability of the water column and prevents deep convection in winter [*Sallée et al.*, 2013a; *Sallée et al.*, 2013b]. This will also affect the carbon exchange with the ocean as active deep convection enhances the rate of carbon uptake [*Sarmiento et al.*, 1998; *Bernardello et al.*, 2014]. CMIP5 projections of future climate, however, show a freshening of the Southern Ocean sea surface, which causes a stronger stratification and eventually a ceasing of deep convection in the Southern Ocean [*de Lavergne et al.*, 2014].

The above CMIP5-based studies mostly discuss the presence and regional consequences of open-ocean deep convection accepting it as part of the modeled mean state under pre-industrial or present-day climate. However, in most models, the deep convection is in fact associated with pronounced variability on an interannual to multidecadal timescale. Simulations with the KCM showed that the variability is key to link the Southern Ocean deep convection to various other processes and quantities of global importance, such as surface air temperature, sea level pressure and associated modes, precipitation, Antarctic sea ice, ocean heat content, meridional density gradient in the ocean, Drake Passage transport, and Atlantic Meridional Overturning Circulation strength [*Park and Latif*, 2008; *Martin et al.*, 2013; *Latif et al.*, 2013; *Martin et al.*, 2015; *Pedro et al.*, 2016]. Motivated by the aforementioned earlier studies indicating significant differences in simulated Southern Ocean deep-convection location, frequency, and intensity among CMIP5 models, we here compare these models with different realizations of the KCM focusing on the deep convection's variability, its timescales, and potential physical controls. For this, we analyze 11 CMIP5 models with prominent deep convection variability and four control simulations of the KCM. From those models, we identify common principles that control Southern Ocean deep-convection variability. In section 2, we describe our methods, models, and experiments, and in section 3, the results are presented. A summary follows in section 4.

2. Method and Models

2.1. Method/Definitions

Our focus in this study is the (re-)occurrence of open-ocean deep convection under stable climate condition. The deep convection is a winter phenomenon. Therefore, we use only the September mean model output from extensive control simulations, most of which were performed using pre-industrial climate conditions. For all models, we calculate the September mixed layer depth by taking the depth of the ocean where the potential density difference to the surface reaches 0.01 kg/m^3. As nearly all models exhibit deep convection in the Atlantic sector of the Southern Ocean, we restrict our analysis to 60°W–60°E and 50°S–70°S. A few models exhibit deep convection also in the Ross Sea or other Southern Ocean regions. The spatial restriction enables us to identify single convection events and their direct interactions. Here we identify deep-convection events through a depth threshold of 3000 m that must be exceeded by the September mixed layer depth. A year is called convective if the integrated area with deep convection covers at least 50,000 km^2 in the Atlantic sector. These definitions are similar to those of *de Lavergne et al.* [2014] but diverge regarding the mixed layer depth defining density difference (they used 0.03 kg/m^3), the region of interest, which we limit to the Atlantic sector, and the deep convection defining thresholds of mixed layer depth (they used 2000 m) and coherent horizontal extent (they chose a minimum of 100,000 km^2). Furthermore, in our analysis, we define a *main convection region* for each model which equals the area in the Atlantic sector where the mixed layer depth exceeds 3000 m for at least 5% of all years provided.

2.2. CMIP5 Simulations

We use pre-industrial control integrations of 11 models from CMIP5 [*Taylor et al.*, 2012]. Our selection omits models that are permanently convecting or never convecting with regard to the mixed layer threshold of 3000 m. We further omit models that provide less than 500 years of output from their pre-industrial control simulation, as the modeled periods associated with deep-convection variability can be multicentennial. The CMIP5 models used in this study are listed in the supporting information Table S1. All of them feature deep convection in the Weddell Sea but only four of them in the Ross Sea.

2.3. Kiel Climate Model Simulations

In our analysis, we also incorporate the KCM, which is a global coupled ocean-atmosphere-sea ice model [*Park et al.*, 2009]. Its components are the ECHAM5 atmosphere general circulation model [*Roeckner et al.*, 2003] and the NEMO ocean-sea ice general circulation model [*Madec*, 2008] coupled by the OASIS3 coupler [*Valcke*, 2006]. In the KCM, no form of flux correction and no anomaly coupling are applied. We use four control experiments to analyze Southern Ocean deep-convection variability. These originate from two versions of the model: Two experiments are conducted with the older version, KCM1.2, which has an atmospheric horizontal resolution of T31 (~3.75°) and 19 vertical levels. The other two experiments are conducted with the KCM1.4 which has a higher atmospheric horizontal resolution of T42 (~2.8°). Furthermore, KCM1.2

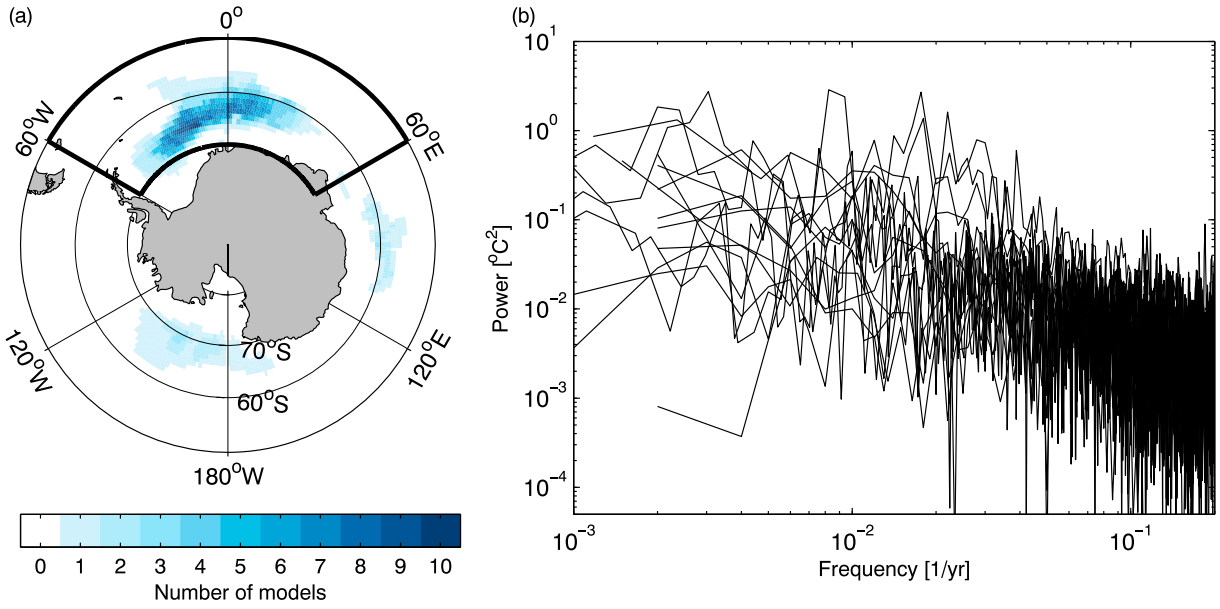

Figure 1. (a) The number of models (out of 15) showing deep convection (according to their "main convection region" defined in section 2.1) at the given grid point. The Atlantic sector of the Southern Ocean (60°W–60°E/50°S–70°S) is marked by the bold black contour line. (b) Power spectra of the September sea surface temperature (SST) index area-averaged over the Atlantic sector from all 15 analyzed models.

and KCM1.4 differ, for example, in the stratus cloud and the oceanic advection schemes and, in certain parameters, specifically those of the sea ice component. Discrepancies in the model results between KCM1.2 and KCM1.4 can thus not be associated with the different grid resolutions conclusively.

The two experiments of the KCM1.2 have both present-day CO_2 concentration and only differ in a single sea ice parameter. This causes a larger amount of sea ice in the KCM1.2b compared to the KCM1.2a [*Martin et al.*, 2013]. The two experiments with the KCM1.4 employ different CO_2 concentration. One uses present-day CO_2 concentration (KCM1.4a) and the other one pre-industrial (KCM1.4b). In all four experiments, the ocean-sea ice model runs on a 2° Mercator mesh with 1.3° on average and an increased meridional resolution of 0.5° close to the equator. The ocean model has 31 vertical levels. The KCM1.2 simulations were used in previous studies (KCM1.2a [*Park and Latif*, 2008, 2010; *Ba et al.*, 2013; *Wu et al.*, 2016] and KCM1.2b [*Martin et al.*, 2013; *Latif et al.*, 2013; *Martin et al.*, 2015]). Details of the KCM experiments are summarized in Table S2. Since the differences in model setup (or external forcing) are comprehensive, we treat the four KCM runs like individual models extending the total number of models to 15. The particular knowledge of the KCM's different setups yields further insight into the physical processes regulating convection variability.

3. Results

In climate models, deep convection is usually not a persistent state but highly variable. A deep winter mixed layer is an indicator for convection events. Therefore, we use the individual *main convection region* of each model as described in section 2.1. All of the 15 models have main convection regions in the Atlantic sector with 10 models agreeing in showing a center in the Weddell Sea (Figure 1a). Only seven models feature additional main convection regions in other parts of the Southern Ocean, four of them in the Ross Sea (supporting information Figure S1). While the specific model setup and mean climate clearly affect the exact location and extent of the deep convection, the Atlantic sector of the Southern Ocean, in the following defined at the area 60°W–60°E/50°S–70°S (black box in Figure 1a), is clearly preferred by the models, and we thus focus our analysis on this region.

During deep convection, the cool surface water mixes with the warmer water below. As a result, deep-convection events are characterized by warm SST anomalies. To measure the periodicity of deep-convection variability, we construct an index by averaging the September mean SST of the Atlantic sector. The frequency power spectrum of the index is visualized in Figure 1b for all 15 models. It reveals red noise characteristics with large differences between the models. Some models exhibit the strongest variability in the

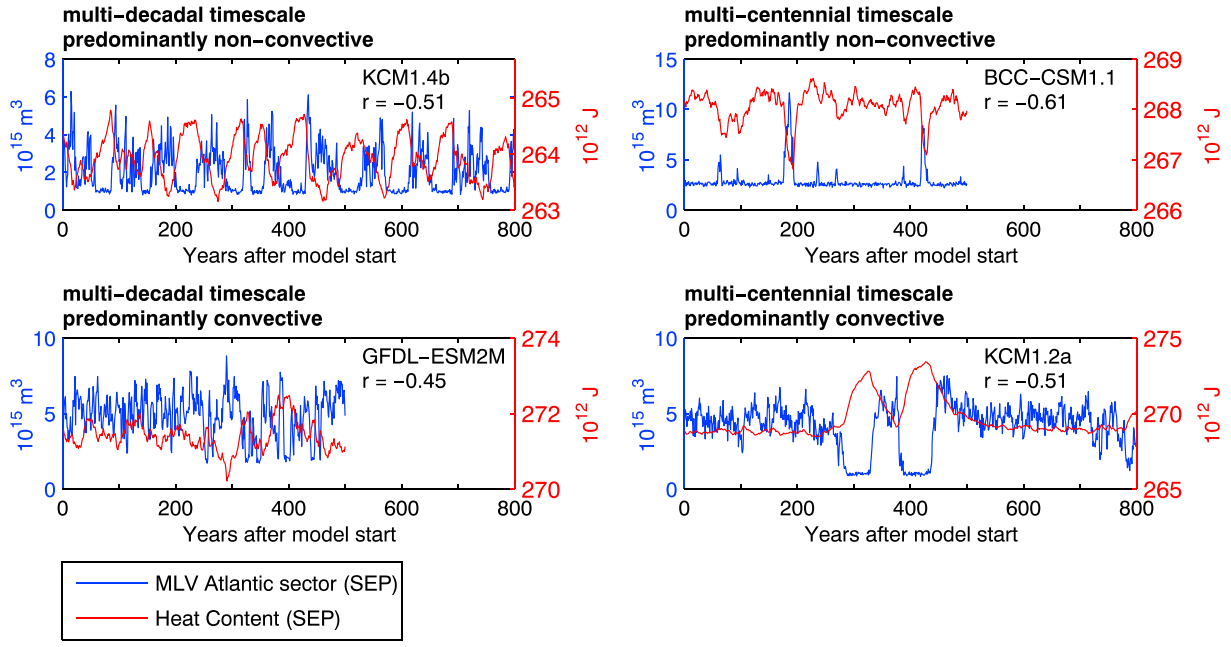

Figure 2. September mean oceanic heat content integrated from 300 to 2000 m and over the Atlantic sector (in red) and the September mixed layer volume (MLV) of the Atlantic sector (in blue). The four models shown here are exemplary for the different characteristics of deep-convection behavior as given in the panel heading. The correlation coefficient (*r*) between the MLV and the heat content is given below the model name. Please note that the ranges of the *y* axes differ.

multicentennial timescale, for example, KCM1.2a and KCM1.2b, others in the multidecadal timescale, such as the GFDL models (Figure S2). Spectra of the Atlantic sector September mean mixed layer volume exhibit very similar peaks (not shown). This supports the notion that the SST variations are indeed associated with deep-convection variability. In some models, pronounced variability due to deep-convection variability appears at multicentennial but also at multidecadal timescales. In general, none of the models exhibits deep-convection variability with a specific constant period. Deep-convection events rather appear within a model-dependent range of timescales.

The onsets and shutdowns of deep convection can be seen in the time series of the September mixed layer volume integrated over the Atlantic sector (blue line in Figure 2) and in the September ocean heat content integrated from 300 to 2000 m over the Atlantic sector (red line). The depth range of 300 to 2000 m approximately covers the model grid levels at which heat is accumulated during periods without convection (Figure S4). In all four exemplary models displayed in Figure 2 (see Figure S3 for all 15 models), the mixed layer volume is anticorrelated to the heat content. *Martin et al.* [2013] investigated the relationship between the Southern Ocean heat content and deep-convection events in KCM1.2a and KCM1.2b: During nonconvective periods, heat that originates from the North Atlantic and enters the Southern Ocean at intermediate depth is accumulated. This warm deep water is also saltier than the sea surface in the Southern Ocean maintaining stability of the water column. Destabilization of the water column results in convective overturning, and the subsurface heat is lost to the atmosphere. Figures 2 and S3 suggest that this process works also in other models than the KCM.

The four models displayed in Figure 2 illustrate the range of different deep-convection behavior that we find in the full model ensemble. The smoother heat content time series (red curve) reveals multidecadal variations in the KCM1.4b and in the GFDL-ESM2M, although the important difference between the two models is that the KCM1.4b remains longer in the nonconvective regime than the GFDL-ESM2M. In contrast, the BCC-CSM1.1 and the KCM1.2a have pronounced multicentennial variability. These two models differ in their convective mean state, as the BCC-CSM1.1 prefers the nonconvective and the KCM1.2a the convective regime. In summary, we find that the models have different timescales and also different tendencies to stay in one regime or the other. The latter can be measured by the percentage of convective years. Thus, the aim of the following analysis is to find the key factors that control the timescale and the percentage of convective years.

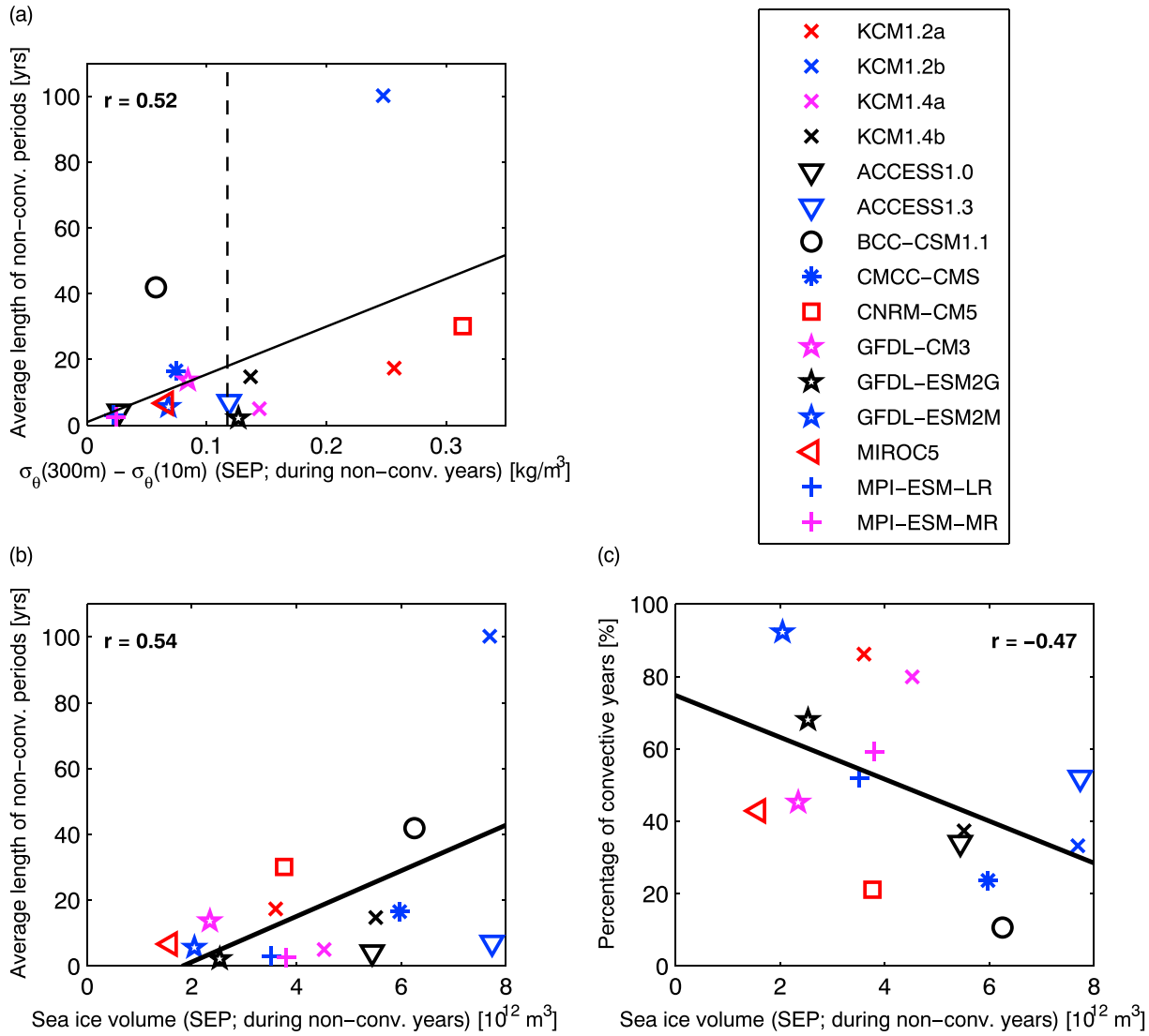

Figure 3. The roles of stratification and sea ice for deep-convection variability based on all analyzed models. (a) Stratification (*x* axis) versus the timescale of deep-convection variability (*y* axis). The stratification is computed as the potential density difference (300 m minus 10 m) of September averaged over the individual main convection regions in the Atlantic sector during years without deep convection. The timescale of variability is here defined as the average number of consecutive nonconvective years (this definition was modulated; the resulting correlation coefficients are listed in Table 1). The dashed black line depicts the observed stratification with some uncertainty, however, as the corresponding convection region is estimated from a single deep-convection event during the years 1974 to 1976. (b) September mean sea ice volume averaged over the Atlantic sector during nonconvective years (*x* axis) versus the timescale of deep-convection variability (same *y* axis as in Figure 3a). (c) September mean sea ice volume (same *x* axis as in Figure 3b) versus the percentage of convective years (*y* axis). The solid black line is the linear regression with the correlation coefficient (*r*) given in one of the upper corners; correlation coefficients that are significant with 90% confidence are given in bold.

Several possibilities exist to define and quantify a characteristic timescale of simulated deep-convection variability. The first possibility is to use the duration of the nonconvective regime, during which heat accumulates in the Weddell Sea region at middepth; a second option is given by the equivalent duration of the convective regime, during which this heat is lost to the atmosphere, and third, one can measure the timescale of the oscillation resulting from shifting between these two regimes. While these measures are not independent, the nonconvective regimes can be distinctly shorter or longer than the convection events and all three timescales are model dependent. We first turn to the nonconvective regime which is terminated by the onset of deep convection. To initiate deep convection, the water column must become unstable. The long-term mean stratification of the ocean is, however, itself closely related to the occurrence of deep convection, which mixes the water masses and thus weakens the stratification. As a measure for the stratification, we show on the *x* axis in Figure 3a the September mean potential density difference between 300 m and 10 m averaged

Table 1. Definitions of the Deep-Convection Timescale and Associated Correlations With the Stratification Strength Averaged Over the Nonconvective Years[a]

Timescale Definition	Correlation Coefficient (With Stratification)
Average length of nonconvective periods (analogous to Figure 3a)	$r = 0.52$
Average length of convective periods	$r = 0.60$
E-folding time of the autocorrelation function of the Atlantic sector heat content 200–3000 m	$r = 0.55$
E-folding time of the autocorrelation function of the Atlantic sector mixed layer volume	$r = 0.65$
E-folding time of the autocorrelation function of the Atlantic sector SST index	$r = 0.66$
Maximum in the power spectrum of the Atlantic sector SST index	$r = 0.41$

[a]These correlations were computed as a test of the relation depicted in Figure 3a (only the definition of the timescale was modulated).

over the individual main convection region during nonconvective years. A large difference reflects a strong stratification. The convective years are excluded as these only show the effect of deep convection, which would be a well-mixed water column with a density difference close to zero. Given the vertical profiles of the potential density that are nearly saturated at a depth of 300 m and do not show any inversions (Figure S4, right), we conclude that the density difference between 300 and 10 m is a robust measure of the models' stratification strength. Also, when the threshold level of 300 m was varied to up to 3000 m, the results changed only slightly. The *y* axis of Figure 3a shows the average length of the nonconvective periods, which is calculated as the average number of consecutive nonconvective years. The resulting average durations are relatively short, because we include even the shortest periods (i.e., single years) in this calculation. Further, we include simulations with different external forcing (e.g., pre-industrial and present day greenhouse gas concentrations) and thus different climate mean state. While this can be assumed to have an impact on the stratification, it should not affect the causal relation that we are testing.

Based on all 15 models, main convection region stratification and duration of nonconvective years are correlated at $r = 0.52$, which is significant at the 90% confidence level (Figure 3a). This means that models with generally weak stratifications tend to have shorter nonconvective periods. This could be explained by the diffusive vertical redistribution of the heat accumulating at middepth, so that average or higher diffusion rates could more easily turn the balance toward the convective regime in these latently unstable models. Similarly, anomalous windy, cold, and dry atmospheric conditions and stronger brine rejection from sea ice formation favor convection in weakly stratified models. However, frequent deep convection continuously erodes the stratification, which hints at a positive feedback acting in such cases. Therefore, it must be stressed that the relation between the timescale and the stratification might be partly established through the effect of the timescale on the stratification. For example, models that stay in the nonconvective regime only for short periods will contain a larger contribution of convection effects in their stratification strength averaged over the nonconvective periods. Nevertheless, choosing a shorter averaging window, e.g., a decade [*Martin et al.*, 2013; *Zanowski et al.*, 2015], to compute a "nonconvective" reference is not applicable to our multimodel analysis, because in 8 of the 15 models the average length of nonconvective periods is shorter than 8 years.

Because there is no straightforward measure for the deep-convection variability timescale, we modified the definition to test the robustness of the relationship with the stratification. The resulting correlation coefficients range between $r = 0.41$ and 0.66 (see Table 1); all are statistically significant with 90% confidence.

Sea ice is a key factor for convection processes because it acts as a lid that moderates the oceanic heat loss to the atmosphere. To initiate strong open-ocean deep convection in winter, a local polynya is crucial to enhance the heat loss. A polynya can form either through divergent winds that mechanically remove sea ice or thermally, through a heat flux from the deeper ocean to the surface [*Williams et al.*, 2007]. We illustrate the relationship between the deep-convection variability and the sea ice volume of September in Figures 3b and 3c (see this relationship for March in Figure S5 and the sea ice seasonal cycle in Figure S6). In Figure 3b September sea ice volume within the Atlantic sector averaged over the nonconvective years is plotted against the average duration of the nonconvective regime (i.e., same *y* axis as in Figure 3a). Again, we exclude the convective years. This largely removes the effect of deep convection which is a reduction in sea ice area and volume in the main convection region. We find a positive correlation between the September sea ice volume and the timescale of the nonconvective periods with a significant coefficient of $r = 0.53$ (Figure 3b). A thick sea ice cover reduces the heat loss from the ocean to the atmosphere and by that protects the surface ocean from too much buoyancy loss, which otherwise could initiate deep convection. If the sea ice extent or

area is used instead of the sea ice volume the correlation becomes insignificant (Table S3), which stresses the importance of the sea ice thickness.

Furthermore, we find that the two control variables, stratification and sea ice volume, are independent. The correlation coefficient for stratification and the September sea ice volume is $r = 0.07$. Two main conclusions can be drawn from the figure: First, strong ocean stratification promotes long periods of inactive deep convection through isolating the heat reservoir below the surface layer from surface interactions that could disturb the stability. Second, a large sea ice cover protects the surface layer from a large buoyancy loss that could initiate deep convection, thereby elongating the phases of inactive deep convection.

Besides the timescale of variability, we find a measure for the models' tendency to prefer the convective regime over the nonconvective. For this, we use the percentage of convective years and contrast it with the September sea ice volume during nonconvective years (Figure 3c). We find a significant anticorrelation of $r = -0.47$. Models with a low (high) sea ice volume tend to stay rather in the convective (nonconvective) regime for two reasons: First, greater sea ice volume is in most cases associated with greater sea ice extent so that deep convection in open water as has been observed in 1974–1976 [*Carsey*, 1980] is inhibited by the ice cover. Second, energy from the warmer subsurface layers is first used to melt the sea ice before major heat loss to the atmosphere can occur, initiating deep convection. By acting as a lid inhibiting direct air-sea fluxes and providing meltwater that stabilizes the surface layer, sea ice prolongs the nonconvective regime and the resulting percentage of convective years is low. For example, the KCM1.2a and the KCM1.2b were implemented with a different sea ice parameter. The total Antarctic sea ice volume in KCM1.2a is 3.6×10^{12} m^3 as opposed to 7.7×10^{12} m^3 in the KM1.2b. As a result, the KCM1.2a exhibits convection 86% of all years but the KCM1.2b only in 33% of all years.

4. Conclusions

Open-ocean deep convection in the Southern Ocean varies considerably among CMIP5 models and different configurations of the KCM regarding location, frequency, intensity, and the percentage of convective years. Based on 15 models with pronounced deep-convection variability, we find stratification strength and sea ice volume to be controlling factors among a variety of climate models which use a wide range of different parameterizations and numerical approaches. The stratification at the convection site influences the timescale of deep-convection variability: Models with a convection site that is weakly stable during the nonconvective years tend to simulate deep-convection variability on shorter timescales than models with a more stable stratification. The presence of sea ice prevents the occurrence of deep convection by freshening the surface when melting and by inhibiting direct heat loss to the atmosphere. In models with a large sea ice volume during nonconvective years, the nonconvective regime dominates. In the 15 models included in our study, deep-convection variability depends critically on the models' mean state. On the one hand, the simulated open-ocean deep convection may be called "spurious" [e.g. *Heuzé et al.*, 2015] as most models overestimate its spatial extent and in many cases also its frequency of occurrence in historical simulations [e.g., *de Lavergne et al.*, 2014]—major open-ocean deep convection was observed only once in the Weddell Sea, and it is unclear whether future climate conditions will allow its re-appearance. On the other hand, the physical mechanism acting in the models producing open-ocean deep-convection oscillations bears intriguing similarities with those of the event in the 1970s. The lack of observations from the pre-industrial era to the mid-20th century makes conclusions about its frequency of occurrence extremely difficult. Our findings can thus define new metrics for model comparison in the Southern Ocean and demonstrate the need for circumpolar sea ice volume estimates from, for instance, remote sensing and intensified observational coverage of the hydrography in deep convection prone regions.

Acknowledgments
We acknowledge the World Climate Research Programme's Working Group on Coupled Modeling, which is responsible for CMIP, and we thank the climate modeling groups for producing and making available their model output. For CMIP the U.S. Department of Energy's Program for Climate Model Diagnosis and Intercomparison (PCMDI) provides coordinating support and led development of software infrastructure in partnership with the Global Organization for Earth System Science Portals. This study was supported by the North Atlantic Climate FP7 Collaborative Project (NACLIM) funded by the European Union, grant agreement 308299, by the InterDec project funded by the German Federal Ministry for Education and Research (BMBF), grant 01LP1609B, and by the National Paleo Climate Modeling Initiative PalMod also funded by the BMBF, grant 01LP1503D. This work was further funded by the Cluster of Excellence 80 "The Future Ocean." The "Future Ocean" is funded within the framework of the Excellence Initiative by the Deutsche Forschungsgemeinschaft (DFG) on behalf of the German federal and state governments. The KCM integrations were performed at the DKRZ Hamburg and the Computing Centre of Kiel University. The KCM data used for this paper can be made available from the authors upon request from W.P. (wpark@geomar.de).

References

Ba, J., N. S. Keenlyside, W. Park, M. Latif, E. Hawkins, and H. Ding (2013), A mechanism for Atlantic multidecadal variability in the Kiel Climate Model, *Clim. Dyn.*, *41*(7–8), 2133–2144, doi:10.1007/s00382-012-1633-4.

Behrens, E., G. Rickard, O. Morgenstern, T. Martin, A. Osprey, and M. Joshi (2016), Southern Ocean deep convection in global climate models: A driver for variability of subpolar gyres and Drake Passage transport on decadal timescales, *J. Geophys. Res. Oceans*, *121*, 3905–3925, doi:10.1002/2015JC011286.

Bernardello, R., I. Marinov, J. B. Palter, E. D. Galbraith, and J. L. Sarmiento (2014), Impact of Weddell Sea deep convection on natural and anthropogenic carbon in a climate model, *Geophys. Res. Lett.*, *41*, 7262–7269, doi:10.1002/2014GL061313.

Carsey, F. D. (1980), Microwave observation of the Weddell polynya, *Mon. Weather Rev.*, *108*(12), 2032–2044, doi:10.1175/1520-0493(1980)108<2032:MOOTWP>2.0.CO;2.
Cook, E. R., B. M. Buckley, R. D. D'Arrigo, and M. J. Peterson (2000), Warm-season temperatures since 1600 BC reconstructed from Tasmanian tree rings and their relationship to large-scale sea surface temperature anomalies, *Clim. Dyn.*, *16*(2–3), 79–91, doi:10.1007/s003820050006.
de Lavergne, C., J. B. Palter, E. D. Galbraith, R. Bernardello, and I. Marinov (2014), Cessation of deep convection in the open Southern Ocean under anthropogenic climate change, *Nat. Clim. Change*, *4*(4), 278–282, doi:10.1038/nclimate2132.
Gordon, A. L. (2014), Southern Ocean polynya, *Nat. Clim. Change*, *4*(4), 249–250, doi:10.1038/nclimate2179.
Heuzé, C., K. J. Heywood, D. P. Stevens, and J. K. Ridley (2013), Southern Ocean bottom water characteristics in CMIP5 models, *Geophys. Res. Lett.*, *40*, 1409–1414, doi:10.1002/grl.50287.
Heuzé, C., J. K. Ridley, D. Calvert, D. P. Stevens, and K. J. Heywood (2015), Increasing vertical mixing to reduce Southern Ocean deep convection in NEMO3.4, *Geosci. Model Dev.*, *8*(10), 3119–3130, doi:10.5194/gmd-8-3119-2015.
Heywood, K. J., et al. (2014), Ocean processes at the Antarctic continental slope, *Phil. Trans. R. Soc. A*, *372*(2019), 20130047, doi:10.1098/rsta.2013.0047.
Jones, J. M., S. T. Gille, H. Goosse, N. J. Abram, P. O. Canziani, D. J. Charman, K. R. Clem, X. Crosta, C. de Lavergne, and I. Eisenman (2016), Assessing recent trends in high-latitude Southern Hemisphere surface climate, *Nat. Clim. Change*, *6*(10), 917–926, doi:10.1038/NCLIMATE3103.
Lara, A., and R. Villalba (1993), A 3620-year temperature record from *Fitzroya cupressoides* tree rings in Southern South America, *Science*, *260*(5111), 1104–1106, doi:10.1126/science.260.5111.1104.
Latif, M., T. Martin, and W. Park (2013), Southern Ocean sector centennial climate variability and recent decadal trends, *J. Clim.*, *26*(19), 7767–7782, doi:10.1175/JCLI-D-12-00281.1.
Madec, G. (2008), *NEMO Ocean Engine*, *Note du Pole de Modélisation*, 396 pp., Institut Pierre-Simon Laplace (IPSL), France.
Martin, T., W. Park, and M. Latif (2013), Multi-centennial variability controlled by Southern Ocean convection in the Kiel Climate Model, *Clim. Dyn.*, *40*(7–8), 2005–2022, doi:10.1007/s00382-012-1586-7.
Martin, T., W. Park, and M. Latif (2015), Southern Ocean forcing of the North Atlantic at multi-centennial time scales in the Kiel Climate Model, *Deep Sea Res., Part II*, *114*, 39–48, doi:10.1016/j.dsr2.2014.01.018.
Orsi, A. H., G. C. Johnson, and J. L. Bullister (1999), Circulation, mixing, and production of Antarctic bottom water, *Prog. Oceanogr.*, *43*(1), 55–109, doi:10.1016/S0079-6611(99)00004-X.
Park, W., and M. Latif (2008), Multidecadal and multicentennial variability of the meridional overturning circulation, *Geophys. Res. Lett.*, *35*, L22703, doi:10.1029/2008GL035779.
Park, W., and M. Latif (2010), Pacific and Atlantic multidecadal variability in the Kiel Climate Model, *Geophys. Res. Lett.*, *37*, L24702, doi:10.1029/2010GL045560.
Park, W., N. Keenlyside, M. Latif, A. Ströh, R. Redler, E. Roeckner, and G. Madec (2009), Tropical Pacific climate and its response to global warming in the Kiel Climate Model, *J. Clim.*, *22*(1), 71–92, doi:10.1175/2008JCLI2261.1.
Pedro, J. B., T. Martin, E. J. Steig, M. Jochum, W. Park, and S. O. Rasmussen (2016), Southern Ocean deep convection as a driver of Antarctic warming events, *Geophys. Res. Lett.*, *43*, 2192–2199, doi:10.1002/2016GL067861.
Roeckner, E., et al. (2003), The atmospheric general circulation model ECHAM5, part I: Model description, Max Planck Inst. for Meteorol. Rep. 349.
Sallée, J. B., E. Shuckburgh, N. Bruneau, A. J. S. Meijers, T. J. Bracegirdle, and Z. Wang (2013a), Assessment of Southern Ocean mixed-layer depths in CMIP5 models: Historical bias and forcing response, *J. Geophys. Res. Oceans*, *118*, 1845–1862, doi:10.1002/jgrc.20157.
Sallée, J. B., E. Shuckburgh, N. Bruneau, A. J. S. Meijers, T. J. Bracegirdle, Z. Wang, and T. Roy (2013b), Assessment of Southern Ocean water mass circulation and characteristics in CMIP5 models: Historical bias and forcing response, *J. Geophys. Res. Oceans*, *118*, 1830–1844, doi:10.1002/jgrc.20135.
Sarmiento, J. L., T. M. C. Hughes, R. J. Stouffer, and S. Manabe (1998), Simulated response of the ocean carbon cycle to anthropogenic climate warming, *Nature*, *393*(6682), 245–249, doi:10.1038/30455.
Taylor, K. E., R. J. Stouffer, and G. A. Meehl (2012), An overview of CMIP5 and the experiment design, *Bull. Am. Meteorol. Soc.*, *93*(4), 485–498, doi:10.1175/BAMS-D-11-00094.1.
Valcke, S. (2006), OASIS3 user guide, *Prism Tech. Rep. 3*, CERFACS, Toulouse, France.
Villalba, R., A. Lara, M. H. Masiokas, R. Urrutia, B. H. Luckman, G. J. Marshall, and C. LeQuesne (2012), Unusual Southern Hemisphere tree growth patterns induced by changes in the Southern Annular Mode, *Nat. Geosci.*, *5*(11), 793–798, doi:10.1038/ngeo1613.
Williams, W. J., E. C. Carmack, and R. G. Ingram (2007), Physical oceanography of polynyas, in *Polynyas: Windows to the World*, *Elsevier Oceanography Series*, vol. 74, edited by W. O. Smith Jr. and D. G. Barber, pp. 55–85, Elsevier, Amsterdam.
Wu, Y., M. Latif, and W. Park (2016), Multiyear predictability of Northern Hemisphere surface air temperature in the Kiel Climate Model, *Clim. Dyn.*, *47*(3), 793–804, doi:10.1007/s00382-015-2871-z.
Zanowski, H., R. Hallberg, and J. L. Sarmiento (2015), Abyssal ocean warming and salinification after Weddell polynyas in the GFDL CM2G coupled climate model, *J. Phys. Oceanogr.*, *45*(11), 2755–2772, doi:10.1175/JPO-D-15-0109.1.
Zunz, V., H. Goosse, and F. Massonnet (2013), How does internal variability influence the ability of CMIP5 models to reproduce the recent trend in Southern Ocean sea ice extent?, *Cryosphere*, *7*(2), 451–468, doi:10.5194/tc-7-451-2013.